Reproductive Development Modulates Gene Expression and Metabolite Levels with Possible Feedback Inhibition of Artemisinin in *Artemisia annua*[1][C][W][OA]

Patrick R. Arsenault, Daniel Vail, Kristin K. Wobbe, Karen Erickson, and Pamela J. Weathers*

Department of Biology and Biotechnology (P.R.A., D.V., P.J.W.) and Department of Chemistry and Biochemistry (K.K.W.), Worcester Polytechnic Institute, Worcester, Massachusetts 01609; Arkansas Bioscience Institute, Arkansas State University, Jonesboro, Arkansas 72401 (D.V.); and Department of Chemistry, Clark University, Worcester, Massachusetts 01610 (K.E.)

The relationship between the transition to budding and flowering in *Artemisia annua* and the production of the antimalarial sesquiterpene, artemisinin (AN), the dynamics of artemisinic metabolite changes, AN-related transcriptional changes, and plant and trichome developmental changes were measured. Maximum production of AN occurs during full flower stage within floral tissues, but that changes in the leafy bracts and nonbolt leaves as the plant shifts from budding to full flower. Expression levels of early pathway genes known to be involved in isopentenyl diphosphate and farnesyl diphosphate biosynthesis leading to AN were not immediately positively correlated with either AN or its precursors. However, we found that the later AN pathway genes, amorpha-4,11-diene synthase (ADS) and the cytochrome P450, CYP71AV1 (CYP), were more highly correlated with AN's immediate precursor, dihydroartemisinic acid, within all leaf tissues tested. In addition, leaf trichome formation throughout the developmental phases of the plant also appears to be more complex than originally thought. Trichome changes correlated closely with the levels of AN but not its precursors. Differences were observed in trichome densities that are dependent both on developmental stage (vegetative, budding, and flowering) and on position (upper and lower leaf tissue). AN levels declined significantly as plants matured, as did *ADS* and *CYP* transcripts. Spraying leaves with AN or artemisinic acid inhibited *CYP* transcription; artemisinic acid also inhibited *ADS* transcription. These data allow us to present a novel model for the differential control of AN biosynthesis as it relates to developmental stage and trichome maturation and collapse.

The medicinal plant *Artemisia annua*, used in traditional Chinese medicine for more than 2,000 years (Acton and Klayman, 1985; Hsu, 2006), produces artemisinin (AN; Fig. 1), the sesquiterpene lactone endoperoxide that is the central component of AN combination therapy. AN combination therapy is currently the most effective malaria drug and is the World Health Organization's currently recommended treatment (Bhattarai et al., 2007). AN also shows promise as a potential therapeutic agent for other parasitic and viral diseases as well as for the treatment of certain cancers and the reduction of angiogenesis (Efferth et al., 2002; Singh and Lai, 2004; Utzinger and Keiser, 2004; Romero et al., 2005). AN has traditionally been isolated from the shoot tissue of field-grown plants, but yield of the drug is characteristically low and does not currently meet worldwide demand. Production through synthetic chemistry, although possible, is not economically feasible. In contrast, certain metabolic engineering approaches appear promising (Ro et al., 2006; Arsenault et al., 2008).

Through the recent work of several groups, the biosynthesis of AN is almost completely elucidated (Fig. 1; Covello et al., 2008). The isopentenyl phosphate (IPP) in AN originates from both the cytosol and plastid arms of the terpenoid biosynthetic pathway (Towler and Weathers, 2007; Schramek et al., 2010). Like all sesquiterpenes, AN is composed of 15 carbons that likely derive from the condensation of three 5-carbon isoprene molecules to farnesyl diphosphate (FPP) by farnesyl diphosphate synthase (*FPS*). Recently, however, Schramek et al. (2010) fed $^{13}CO_2$ to *A. annua* plants and obtained labeled artemisinic intermediates, which suggested that FPP may instead be condensing a geranyl diphosphate of mixed IPP origin with a cytosolic IPP. FPP is converted to amorpha-4,11-diene through the activity of amorpha diene synthase (*ADS*; Bouwmeester et al., 1999; Picaud et al., 2005).

[1] This work was supported by the National Institutes of Health (grant nos. 2R15GM069562–02 and 2R15GM069562–03), by the Arkansas Biosciences Institute, the major research component of the Arkansas Tobacco Settlement Proceeds Act of 2000, and by the Worcester Polytechnic Institute and the George Alden Trust to P.R.A.

* Corresponding author; e-mail weathers@wpi.edu.

The author responsible for distribution of materials integral to the findings presented in this article in accordance with the policy described in the Instructions for Authors (www.plantphysiol.org) is: Pamela J. Weathers (weathers@wpi.edu).

[C] Some figures in this article are displayed in color online but in black and white in the print edition.

[W] The online version of this article contains Web-only data.

[OA] Open Access articles can be viewed online without a subscription.

www.plantphysiol.org/cgi/doi/10.1104/pp.110.162552

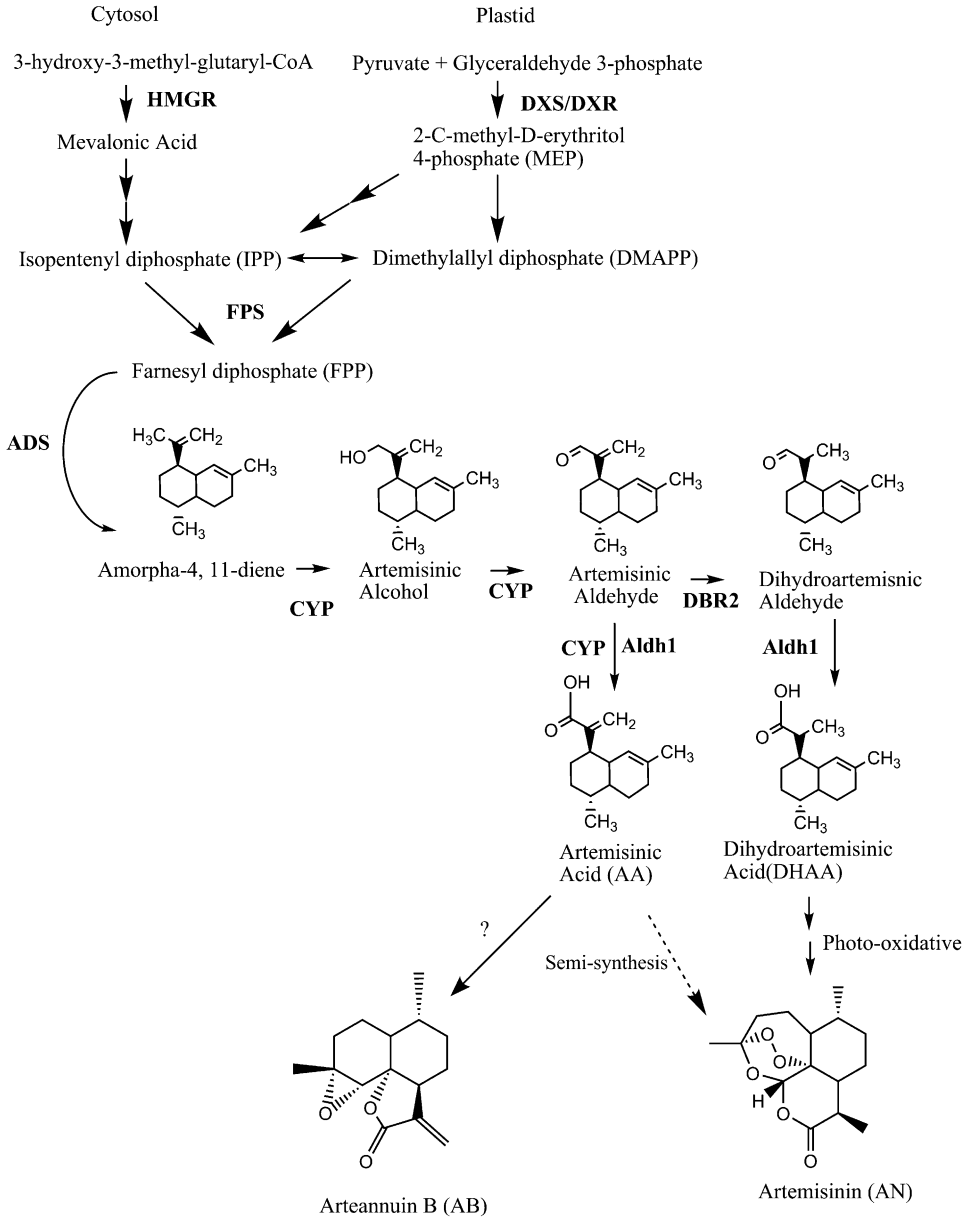

Figure 1. Isopentenyl diphosphate and AN biosynthetic pathway. MEP, Nonmevalonate pathway (plastid pathway).

Amorpha-4,11-diene is subsequently oxidized in three steps to artemisinic acid (AA) through the action of a single enzyme, CYP71AV1 (CYP; Ro et al., 2006; Teoh et al., 2006). Recently a double bond reductase (*DBR2*; Zhang et al., 2008) and an aldehyde dehydrogenase (*Aldh1*; Teoh et al., 2009) were also isolated (Fig. 1). They appear to function in the conversion of artemisinic aldehyde to its dihydro form and then to dihydroartemisinic acid (DHAA), respectively; Aldh1 appears to also convert artemisinic aldehyde to AA, an activity also ascribed to CYP (Zhang et al., 2008). AA may then be converted to either arteannuin B (AB) or potentially to DHAA and then to AN (Sy and Brown, 2002; Brown and Sy, 2007; Fig. 1). The mechanisms of these final steps are not currently known, but it has been suggested that they may be the result of a nonenzymatic, photooxidation reaction (Sy and Brown, 2002). Many of these genes are highly expressed in glandular trichomes, from whose cDNA libraries they were cloned (Zhang et al., 2008, 2009; Teoh et al., 2009).

AN is produced in 10-cell glandular trichomes located on leaves, floral buds, and flowers (Ferreira et al., 1995; Tellez et al., 1999; Olsson et al., 2009) and sequestered in the epicuticular sac at the apex of the trichome (Olsson et al., 2009). The two apical secretory cells lack chlorophyll, but likely have other colorless plastids. The four secretory cells beneath the apical cells, however, have chlorophyll and seem to have fully functional chloroplasts. In nonflowering *A. annua*

plants (i.e. during vegetative growth), trichome numbers increased per unit area on the adaxial leaf surface until leaf expansion ceased, at which point trichome numbers began to decline, apparently a result of their collapse (Lommen et al., 2006); to our knowledge, no data have been reported for changes in trichome counts on the abaxial leaf surface, for floral bolt leaves (the leafy bracts), or in relation to the epidermal cells. Lommen et al. (2006) further observed that AN levels, which rise with increasing trichome numbers, continue to rise even after trichome populations begin collapsing. They attributed the increase in AN to maturation effects within the trichome. Recently, Olsson et al. (2009) used laser-dissected trichomes to show that transcripts of genes for AN biosynthetic enzymes post FPP, ADS, CYP, and DBR2 were present in the two apical cells but not in the four subapical cells of the glandular trichomes. On the other hand, transcripts of 1-deoxyxylulouse 5-phosphate reductoisomerase (DXR), a plastid-localized (Fung et al., 2010) enzyme, were not present in the apical cells but were found in the remainder of the trichome. FPS transcripts were found throughout the trichome.

Many studies have shown that AN content can vary widely among different cultivars or ecotypes of *A. annua* (Wallaart et al., 2001). It has also been reported that AN content is responsive to the time of harvest, light intensity, and developmental stage (Ferreira et al., 1995). Specifically regarding developmental stage, AN levels are reported to reach their peak either just before flowering or at full flower (Acton and Klayman, 1985; Woerdenbag et al., 1993). Flowering, however, may not be necessary for increasing AN content, as plants transformed with the flower-promoting factor 1 were induced to flower much earlier but did not produce significantly increased levels of AN (Wang et al., 2004). Consequently, other factors linked to the reproductive developmental phase change are likely more involved in increasing AN levels.

To provide more insight into the regulation of AN biosynthesis in *A. annua*, this study measured changes in steady-state mRNA levels, trichome populations, and artemisinic metabolite levels in response to the shift in *A. annua* from the vegetative to the reproductive growth phase (Fig. 2). Transcripts of six key genes in AN biosynthesis were measured: 3-hydroxy-3-methyl-glutaryl-CoA reductase (*HMGR*) from the cytosolic mevalonic acid-dependent IPP pathway, 1-deoxyxylulose 5-phosphate synthase (*DXS*) and *DXR* from the plastidic mevalonate-independent IPP pathway, *FPS*, *ADS*, and *CYP*. Leaf trichome populations and the levels of AA, DHAA, AB, and AN were also measured.

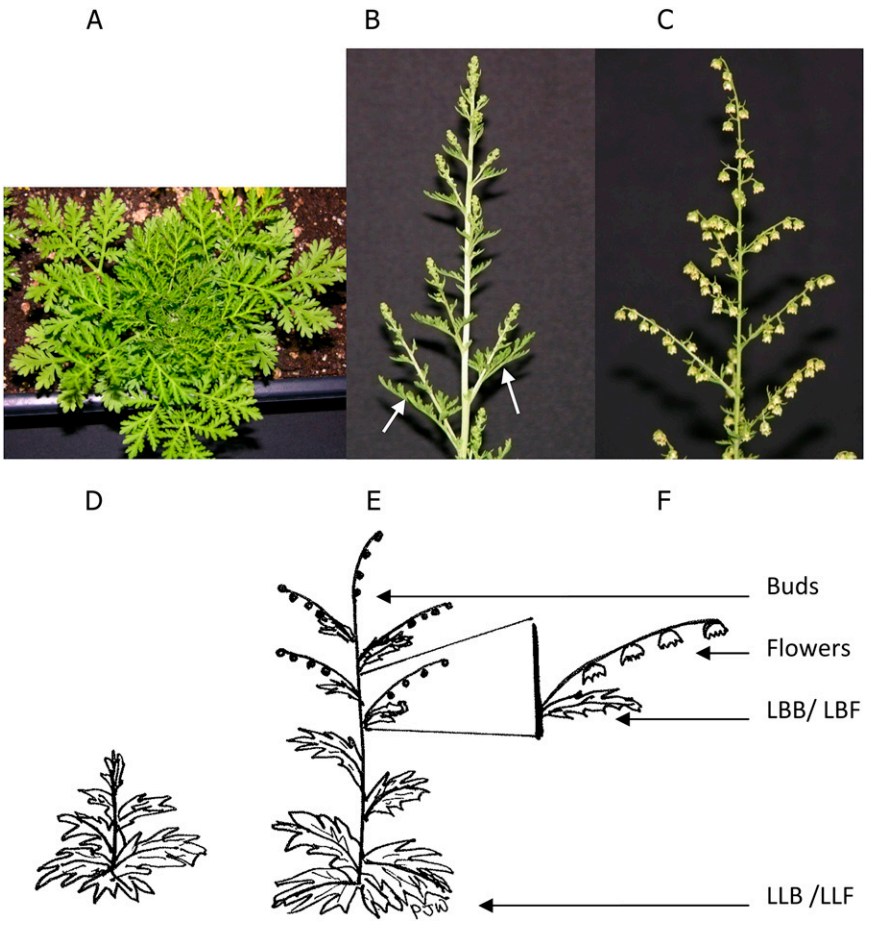

Figure 2. *A. annua* during vegetative and reproductive growth. A, Vegetative growth. B, Floral bolt developed. C, Full flower. Arrows indicate the leafy bracts. D to F, Schematic of locations of leaves of different ages on vegetative plants (D), on budding plants (F), and on plants in full flower (F). [See online article for color version of this figure.]

RESULTS

While others (Acton and Klayman, 1985; Woerdenbag et al., 1993) demonstrated that increases in AN occur with the transition from vegetative growth to the reproductive cycle in *A. annua*, little is known about the effects this transition has on other artemisinic metabolites or on the transcriptional activity of key genes in the AN pathway. Seven tissues were analyzed for transcripts and the AN metabolites, AN, AA, AB, and DHAA: leaves of vegetative plants (VEG), flower buds (BUD), fully open flowers (FLW), leafy bracts from the floral bolts of budding (LBB) and full-flowering (LBF) plants, and the large leaves below the bolts of budding (LLB) and full-flowering (LLF) plants. Comparisons were made between shifting metabolite concentrations, leaf trichome populations, and alterations in the transcription of relevant genes for plants transitioned from vegetative to reproductive growth.

Artemisinic Metabolite Profiles

All parts of reproductive plants showed equal or greater amounts of AN than vegetative leaves (Fig. 3). AN was highest in flowers at 1.16 mg g^{-1} fresh weight during anthesis and more than 10-fold greater than that observed in either vegetative leaves or in floral buds (Fig. 3). As plants shifted from vegetative growth to reproductive growth, the AN levels of the large vegetative leaves on the plant increased from 0.12 mg g^{-1} fresh weight in the VEG leaves to 0.59 mg g^{-1} fresh weight in the LLF tissues (Fig. 3, VEG→LLB→LF). In contrast, the AN content of the smaller leafy bracts decreased more than 3-fold once flowers fully developed (Fig. 3, LBB→LBF).

A similar distribution pattern for AB was also observed (Fig. 3). Again, every tissue type from reproductive plants showed higher levels than leaves from vegetative plants. Within the reproductive plants, the pattern of AB production was almost identical to that observed for AN (Fig. 3). The highest levels were once again observed in FLW (1.94 mg g^{-1} fresh weight) followed closely by LBB (1.38 mg g^{-1} fresh weight); BUD and the LBF had concentrations of AB at 0.28 and 0.45 mg g^{-1} fresh weight, respectively. This was only marginally more than the amount found in vegetative leaves (Fig. 3). As the floral buds expanded to full flower, the AB levels increased about 7-fold (Fig. 3, BUD→FLW). Although the large leaves beneath the bolt increased slightly in AB concentration during this transition to full flower, AB in the leafy bracts decreased about 3-fold (Fig. 3).

When the amounts of the two precursor compounds, AA and DHAA, were measured, a pattern different from either AB or AN emerged (Fig. 3). VEG showed the highest level of either metabolite, at 0.54 mg AA g^{-1} fresh weight and 0.52 mg DHAA g^{-1} fresh weight, and these levels decreased substantially during floral bud formation and full flowering (Fig. 3, VEG→LLB→LLF). AA similarly declined in these tissues, but to a lesser degree (Fig. 3, VEG→LLB→LLF). Reproductive phase tissues showed nearly uniform low levels of both DHAA and AA except for the LBB, which showed about twice as much DHAA as any other tissue in reproductive phase plants. It is also interesting that in vegetative leaves, the levels of AN and AB were much lower than their respective precursors, DHAA and AA (Fig. 3).

Transcript Analysis

To determine if transcript levels correlated with measured metabolite levels, tissue samples from vegetative, budding, and flowering plants were harvested and separated into their constitutive parts for analysis by real-time reverse transcription (RT)-PCR. Sample transcript levels were standardized to 18S rRNA and compared relative to vegetative plants. Six major genes were measured. They represent the mevalonic (*HMGR*) and nonmevalonic (*DXS* and *DXR*) pathways for IPP production, sesquiterpene-specific IPP condensation (*FPS*), and two artemisinic metabolite-specific transcripts (*ADS* and *CYP*).

Interestingly, the changes in transcript levels for the studied genes in these tissues varied by more than 3 orders of magnitude (Fig. 4). The genes that showed the least variation in transcript levels from vegetative leaves were the two nonmevalonic pathway genes, *DXS* and *DXR*. These both showed peak expression

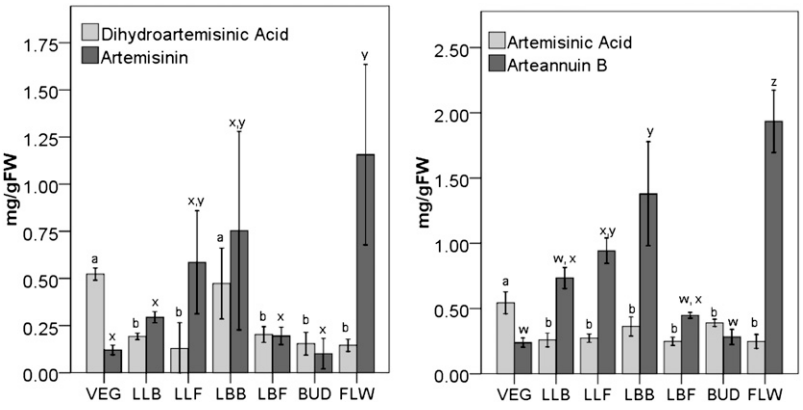

Figure 3. Artemisinic metabolite response to budding and flowering. Metabolites were extracted from fresh plant material and assayed by liquid chromatography-mass spectrometry. Letters show statistical significance for each metabolite; values are means ± SD ($n = 3$). FW, Fresh weight.

only about 6-fold higher in buds and approximately 4-fold higher in leafy bracts relative to vegetative tissue. Similarly, in floral buds, *HMGR* and *FPS* showed peak transcript levels at 27- and 10-fold higher than in vegetative tissues, respectively. The AN-specific genes, *ADS* and *CYP*, showed dramatic declines in transcription relative to vegetative tissue, with transcript levels in some tissues more than 100-fold below that in vegetative tissue in all tissues except buds, which showed significant increases.

In looking for patterns of expression, it can be seen that, in general, the lower leaves showed minimal changes in gene expression, except for the AN pathway-specific genes, which showed dramatic declines in expression in these tissues (Fig. 4). The bract leaves had higher levels of transcripts during budding and less at flowering for all genes tested except *FPS*, which showed no change. A similar pattern was seen for the floral buds; all transcript levels decreased at full flower.

Trichome Levels

AN is produced and stored in the glandular trichomes on *A. annua* plants, so trichome populations were measured on different leafy tissues taken from plants in each developmental phase. In leaves from vegetative plants, the number of trichomes in relation to epidermal cells was highest when the leaves were young and then declined significantly once leaves were fully expanded (Supplemental Fig. S1). This suggests that trichomes are actually eliminated or collapsed rather than just reduced in relative number

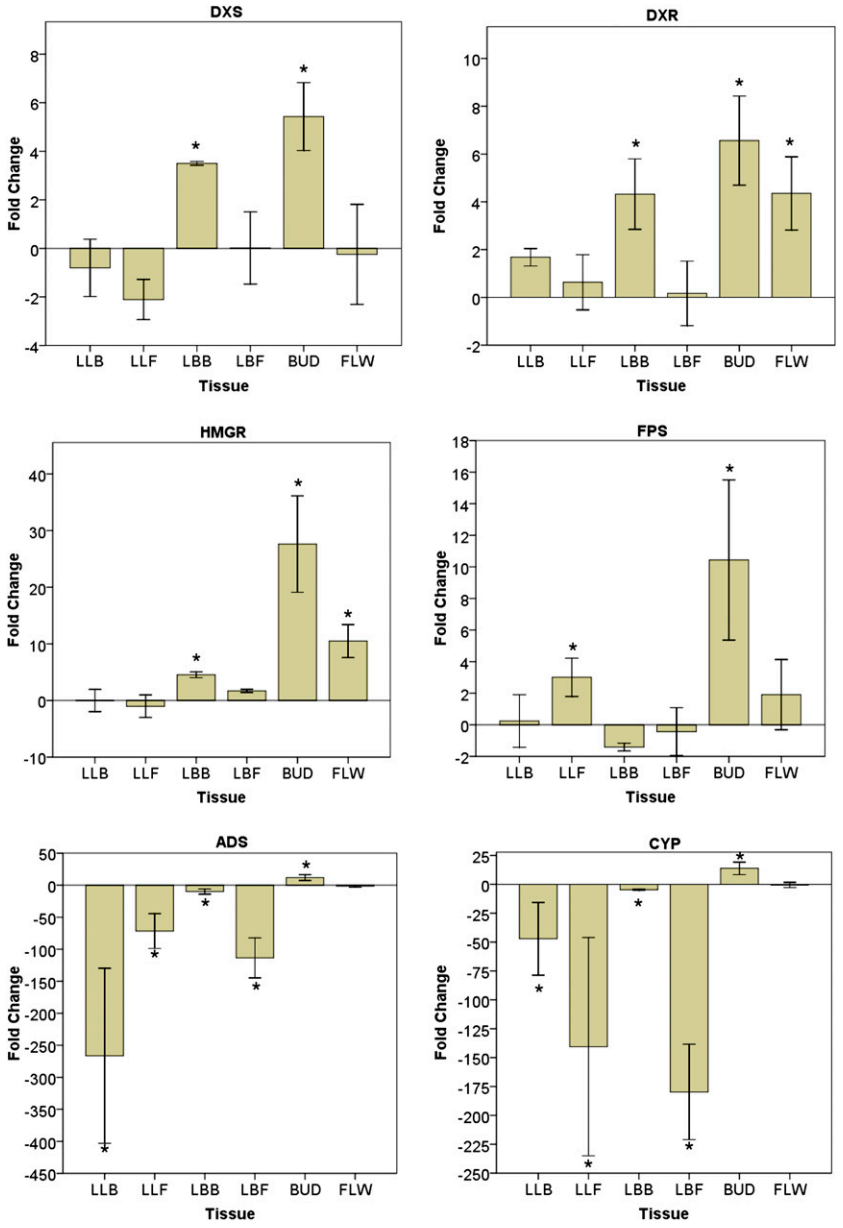

Figure 4. Responses of artemisinic metabolite-specific genes (*DXS*, *DXR*, *HMGR*, *FPS*, *ADS*, and *CYP71AV1*) to budding and flowering. Values displayed are mean fold change as calculated by the $2^{-\Delta\Delta CT}$ method ± SD ($n = 5$). * $P < 0.05$, relative to vegetative plants. [See online article for color version of this figure.]

per unit area as cells expand. The nonbolt leaves (LLB or LLF) on reproductive plants (Fig. 2, E and F) have a significantly greater trichome-to-epidermal cell ratio than the oldest leaves on vegetative plants; trichome numbers per 1,000 epidermal cells are 141.2 (flowering plants), 70.7 (budding plants), and 41.22 (vegetative plants; Supplemental Fig. S1).

In contrast, the youngest leaves from both vegetative- and reproductive-stage plants showed no significant difference in their trichome-to-epidermal cell ratio (compare ULV with LBB with LBF). However, the number of trichomes mm^{-2} did increase significantly in the adaxial population of the youngest leaves of budding and flowering plants relative to vegetative plants. Trichome populations (number mm^{-2}) showed close correlation with AN and AB content of each type of leaf analyzed (Fig. 5).

Exogenous AN and AA Affect AN-Related Transcript Levels

Lommen et al. (2006) previously suggested that, upon maturation, trichomes collapse. We considered that this could in turn release the sequestered AN and possibly exert feedback control on AN production. This hypothesis was tested by spraying mature vegetative plants with either AN or AA in 70% ethanol (100 $\mu g\ mL^{-1}$). Compared with 70% ethanol controls, AN-sprayed plants showed no change in transcripts for *HMGR*, *FPS*, and *ADS* (Fig. 6). *CYP*, however, showed a greater than 10-fold decline. Plants sprayed with AA also showed no significant change in transcripts of *HMGR* and *FPS*; however, *ADS* and *CYP* decreased 10- and 5-fold, respectively (Fig. 6).

DISCUSSION

Similar to some earlier accounts (Ferreira et al., 1995), the highest levels of AN in the *A. annua* 'YU'

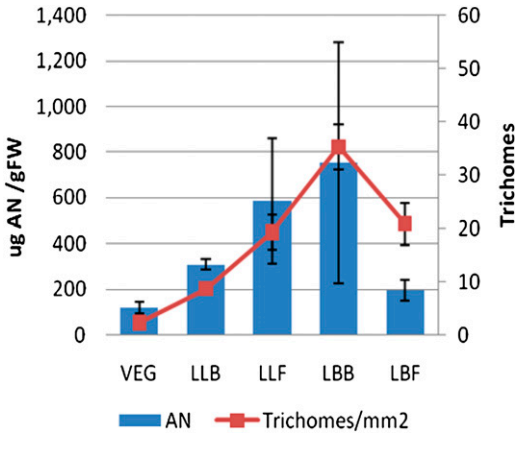

Figure 5. AN levels correlate with trichome densities regardless of leaf type. Bars show AN content in various leaf types. Points represent total glandular trichome (adaxial + abaxial) populations. Error bars represent SD. FW, Fresh weight. [See online article for color version of this figure.]

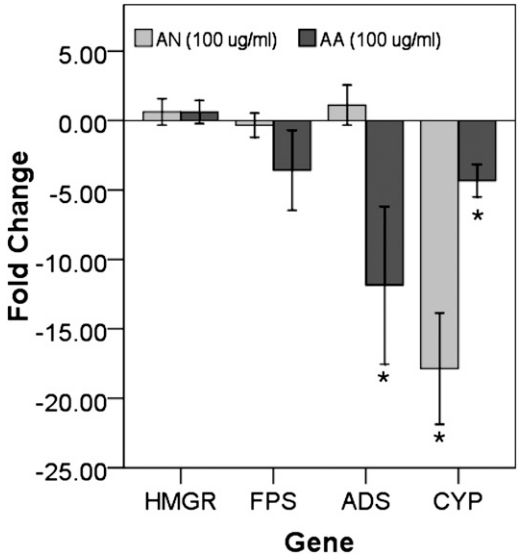

Figure 6. Changes in gene expression with spraying of 50 $\mu g\ mL^{-1}$ AN in 70% ethanol relative to spraying with 70% ethanol controls. Asterisks show significant differences at $P \leq 0.05$ ($n = 4$).

occurred during anthesis in flowers. Wang et al. (2004) had already shown that flower formation was not necessary for increasing the content of AN in *A. annua*, so other aspects of this developmental phase change were investigated: changes in metabolite and transcript levels and trichome populations. These changes, from the vegetative stage to the budding stage to anthesis, are summarized in Figure 7.

The various chemotypes that exist in *A. annua* are most often distinguished by the metabolite balance between AN/DHAA and AB/AA (Wallaart et al., 2001). For example, similar to our results, Zhang et al. (2005), using the 001 strain of *A. annua*, found that AN peaked at full bloom while AA content decreased during the transition from the vegetative to the reproductive stage. On the other hand, Ma et al. (2008) showed, using the same 001 strain, that peak levels of AN occurred more or less throughout the entire flowering stage from bolt initiation to full flower; AA dropped substantially as the bolt began to develop but rose somewhat at full flower. As the wild-type 001 strain transitioned from vegetative growth to full flower, the AN/DHAA ratio was similar to our results. In contrast, the AB/AA ratio remained stable. Together, these data underscore the hypothesis that different subpopulations exist with variations in the temporal and tissue distribution of these metabolites and that, quite simply, the debate over when the highest level of AN occurs may be due to cultivar selection and to when and which tissues are selected for extraction.

AN and AB are believed to be the terminal products of the pathway and generally increase throughout development; this is seen in the lower leaves and in the buds and flowers. However, the leafy bracts show a

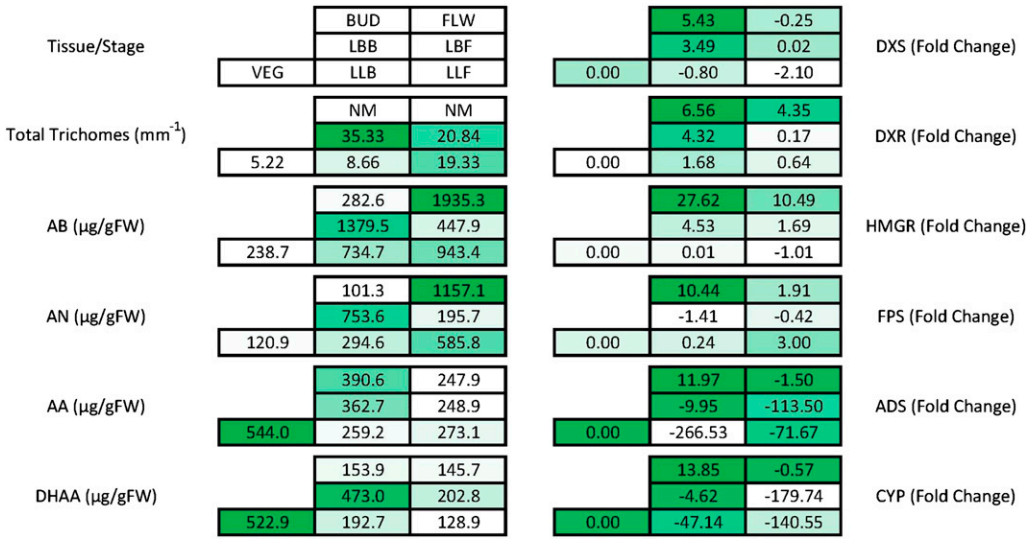

Figure 7. Summation of trichome populations, transcript levels, and artemisinic metabolites throughout the development of *A. annua* from vegetative growth through full flowering. Numbers within each box are average values obtained for each leaf type analyzed for the indicated factor. Shading of the boxes indicates the relative level of response. Fold change is against VEG leaves. FW, Fresh weight. [See online article for color version of this figure.]

distinctly different pattern. In these tissues, AN, AB, AA, and DHAA concentrations are higher during budding than flowering. This leads to the obvious question of the fate of these compounds during that transition: are they converted to other secondary metabolites, transported to other tissues, or released to the environment? The decline in AN and AB, as well as the decline in *ADS* and *CYP* transcripts, may be related to collapsing trichome populations and feedback inhibition by AN as it is released from the epicuticular space.

In *A. annua*, breeding for increased trichome number results in increased AN levels (Graham et al., 2010), which is consistent with our data. In Arabidopsis (*Arabidopsis thaliana*), the density of trichomes on epidermal tissues undergoes major changes with plant maturation and then again with the transition to reproductive growth (Chien and Sussex, 1996; Telfer et al., 1997). A similar pattern of change in trichome distribution may help explain the patterns of AN concentration observed here. Although trichome counts have been reported for *A. annua*, data were obtained only from the adaxial surface of leaves and apparently only from plants in the vegetative phase of growth (Lommen et al., 2006; Liu et al., 2009). Likewise, instead of correlating trichome numbers to their neighboring epidermal cell population, counts have been generally reported as trichomes per unit leaf area and range from 20 to 80 trichomes mm^{-2}, the number usually declining with leaf maturity (Lommen et al., 2006) although increasing with plant age (Lommen et al., 2006; Liu et al., 2009). Additionally, studies have typically focused on only the adaxial surfaces and the youngest leaves on a given plant, which have the highest density of trichomes. In contrast, we measured trichome populations with regard to leaf position, developmental stage, and both adaxial and abaxial surface changes. Vegetative plants in our study showed similar trichome population dynamics for adaxial surfaces, with 11.8 ± 1.25 and 1.2 ± 0.2 (mean ± SE) trichomes mm^{-2} for young versus mature leaves, respectively. In addition, the numbers on the adaxial and abaxial surfaces were quite similar for a given leaf type.

Trichome maturation from LLB to LLF tissues could explain the increases in AN content, as trichomes increase in size and density and subsequently allow for the conversion of DHAA or AA to AN or AB, respectively. As glandular trichomes mature, their fragility increases and eventually they burst; younger trichomes with less expanded cuticles are more stable (Lommen et al., 2006). This would help explain the decreases seen in the LBB→LBF transition, both in transcript abundance and in AN levels. The trichomes on the leafy bracts on budding plants are quite young, so they are able to accumulate and sequester AN effectively; thus, putative feedback to *CYP* would be somewhat mitigated, despite the high AN levels that were measured. As these same leaves transition to the full flower stage, trichomes begin to disappear, possibly breaking and releasing their contents.

Exogenous AN has the ability to inhibit primary root elongation in seedlings (Arsenault et al., 2010), so it is capable of influencing intracellular processes even when presented extracellularly. The rupture or senescence of trichomes and the release of AN or possibly other downstream metabolites from the epicuticular trichome sack to the surroundings probably accounts for the greater than 100-fold decrease in *CYP* and *ADS* transcript levels measured at this stage. This appears to be the case, since leaves sprayed with AN

show significant decreases in *CYP*, suggesting that there is some feedback inhibition by AN on the *CYP* gene. Interestingly, AN does not seem to have a significant effect on *ADS*; instead, AA inhibits *ADS* while also inhibiting *CYP*. However, it should be noted that the concentration used to show the inhibitory effects would lie well within the lower range of concentrations present in mature trichomes and that higher concentrations may show more dramatic effects.

Relative to vegetative plants, the responses of six genes in this study can be categorized into two broad groups based on the expression patterns they exhibited during the transition to reproductive growth. The non-AN-specific genes (*DXS*, *DXR*, *HMGR*, and *FPS*) showed their peak expression in bud tissue followed by progressively lower expression in floral tissue (BUD > FLW > VEG), with lowest expression in the leafy bracts (Fig. 8). In the leafy bracts, *DXS*, *DXR*, and *HMGR* were significantly greater than vegetative leaves, but only during budding.

Transcript levels of *FPS*, on the other hand, are highest during flowering, coinciding with maximum AN levels. *FPS* transcript levels are of particular interest because Chen et al. (2000) showed that in transgenic *A. annua* expressing enhanced levels of *FPS*, AN levels also increased two to three times above nontransgenic controls, an observation consistent with our results. Interestingly, however, Ma et al. (2008) also overexpressed *FPS* but did not observe increases in AN.

The second group of AN metabolite-specific genes (*ADS* and *CYP*) seemed to show a very different pattern of expression, in which budding correlates with large decreases in transcripts in the leafy bracts while buds have comparatively high levels of these transcripts. Previously, Zhang et al. (2006) showed large amounts of AN in flowers, so the increase in AN-specific gene expression was anticipated in buds and occurred prior to the peak levels of AN and AA. This suggests that the large decrease in AN- and AA-specific transcripts (*ADS* and *CYP*) in flowers may be related to negative feedback, where both AN and AA production are regulated through the repression of transcription of *CYP* and/or *ADS*. AN is known to be phytotoxic (Duke et al., 1987; Arsenault et al., 2010), so this putative feedback mechanism could limit the production of this toxic metabolite.

When examining the effects of decreasing transcript levels, it is important to compare similar tissues across multiple time points. Decreases observed in the lower nonbolt leaves of both budding and flowering plants relative to vegetative plants correlated well with the relative amounts of DHAA observed in these tissues. If only leaves are considered, *CYP* transcripts showed decreasing abundance from that in the vegetative and vegetative-related leaves to those on the leafy bracts as the plant shifted from vegetative to budding to flowering: VEG > LBB > LLB > LLF > LBF. The levels of DHAA, a downstream product of *CYP* activity, showed an identical trend of decreasing abundance in the same tissues. Generally, *ADS* transcript levels followed a similar trend.

Bud and flower tissues, on the other hand, present a more complex scenario for AN production; transcripts for both *ADS* and *CYP* either increase (BUD) or stay constant (FLW) relative to VEG leaves. Buds showed an increase in transcripts of *ADS* and *CYP* as well as the early pathway genes *HMGR*, *FPS*, *DXR*, and *DXS*. This response probably indicates a ramp up in production of numerous terpenoid products that are key components of the essential oils often prevalent in floral tissues. The subsequent decrease in *CYP* and *ADS* transcript levels at full flower is consistent with AN acting to regulate its own biosynthesis at the level of these enzymes and correlates well with our data showing inhibition of *ADS* and *CYP* by AN and AA.

A recent gene expression study in *A. annua* by Liu et al. (2009) used the *A. annua* 'H050139'. Their work showed little to no change in *FPS* or *CYP* levels, whereas our study found large decreases in both transcript levels accompanying the transition from floral bud to full flower. Although their results for *DXR* are similar to ours, they showed more *ADS* transcripts in flowering plants relative to budding plants than we observed. The differences between their study and ours may be attributable to variations in clonal populations and the previously established existence of chemotypes within this species (Wallaart et al., 2001).

The levels of AN in leaf tissues correlated quite well with the relative number of trichomes mm^{-2}. Liu et al. (2009) reported a correlation coefficient between

Table I. *Significant data correlations (r^2) and P values between factors at $P \leq 0.05$*

Correlation values are shown above dashes, while *P* values are shown below. NS, Not statistically significant.

	ADS	*CYP*	Trichome No.	AA	DHAA	AB	AN
ADS	–	0.91	NS	0.98	0.89	NS	NS
CYP	0.03	–	NS	0.93	0.96	NS	NS
Trichome No.	NS	NS	–	NS	NS	0.98	0.99
AA	0.003	0.02	NS	–	0.89	NS	NS
DHAA	0.04	0.01	NS	0.044	–	NS	NS
AB	NS	NS	0.005	NS	NS	–	0.98
AN	NS	NS	0.002	NS	NS	0.0036	–

the density of glandular trichomes and AN content of 0.987; application of methyl jasmonate to plants doubled the trichome count and the AN concentration. Our results showed a similar close correlation between trichome number and AN throughout budding and flowering (Table I). Furthermore, the downstream putative end products, AN and AB, showed a high correlation with trichome density, while their precursor molecules, DHAA and AA, were instead better correlated with *ADS* and *CYP* transcript abundance (Table I). This is likely explained by a feedback mechanism acting on *CYP* and/or *ADS* expression, limiting production of the relatively more polar AA and DHAA. The more hydrophobic AN and AB, on the other hand, may be largely sequestered to glandular trichomes, where their phytotoxic effects are limited; thus, their ability to affect transcription also may be limited. Olsson et al. (2009) suggested that this is the case at least for AN; when present in the growth medium, levels far below those measured in these tissues (50 μg mL^{-1} or greater) are sufficient to inhibit 75% or more of root elongation in *A. annua* seedlings (Arsenault et al., 2010). Sy and Brown (2002) showed that DHAA may undergo spontaneous autooxidation in highly lipophilic environments, which lends support to the notion that the final conversion of DHAA to AN may occur within the subcuticular space of the glandular trichome, where hydrophobic AN appears to be sequestered. In the above scenario, bursting of the outermost cuticular layer due to mechanical stress or age would allow for AN to be released.

Overall, only *ADS* and *CYP* genes showed significant correlations with any of the metabolites or trichomes (Table I). There were no significant correlations between *HMGR*, *FPS*, *DXS*, and *DXR* with any of the measured artemisinic metabolites or trichome populations. *ADS* and *CYP* expression correlated well with the precursors, AA and DHAA, throughout development, but not with their respective end products, AB and AN (Table I). This is consistent with the apparent feedback inhibition that AA exerts on both genes. Trichome number, on the other hand, showed a high correlation with both AN and AB levels but not with their respective precursors, DHAA and AA (Table I). These are end products of two branches of the AN pathway; thus, this correlation is consistent with the storage role of the trichome for at least AN and possibly also AB.

CONCLUSION

To our knowledge, this is the first report correlating the transcription of six key genes involved in AN biosynthesis, artemisinic metabolite levels, and trichome populations with *A. annua* growth phase. Significantly, changes in trichome numbers correlated well with AN/AB content of a given leaf type (i.e. lower leaves steadily increased the amount of AN/AB and simultaneously showed a steady increase in trichome number). Precursor concentrations did not show this correlation. Although evidence is presented that supports a negative feedback loop of AN and AA on *ADS* and *CYP* genes, other transcript levels do not correlate well with AN production, suggesting that control is not maintained through transcription alone.

MATERIALS AND METHODS

Plant Growth Conditions

Artemisia annua 'YU' (isolated from the former Yugoslavia; a gift of Nancy Acton, Walter Reed Army Institute of Research) was grown from seed in growth chambers maintained at 28°C with a light intensity of approximately 90 μmol m^{-2} s^{-1}. Plants were grown in Metromix 360 soil (Sungro) in 12- × 12- × 5-cm pots, and all plants received regular watering and biweekly fertilizer treatments. Plants were maintained in a vegetative state (Fig. 2) through a long-day photoperiod of 16 h of light and 8 h of dark. After 8 weeks, when plants reached a height of approximately 15 cm, a random subset of developmentally consistent plants was selected and moved to a growth chamber with identical environmental conditions, but with 8 h of light and 16 h of dark. Floral bolts were observed about 18 d later (Fig. 2).

Plants were allowed to develop full flowers and harvested 1 d later. Vegetatively grown plants were harvested after the same period of growth as those in full flower, approximately 13 weeks after planting. At harvest, plant stems and roots were discarded and the rest of the plant material was separated as follows for extraction and analysis: leaves from vegetatively grown plants (VEG); from reproductive plants during floral budding, leafy bracts (LBB) and floral buds (BUD) off the floral bolts and the large leaves below the bolt (LLB); from reproductive plants during full flower, leafy bracts (LBF) and flowers (FLW) off the floral bolt and the large leaves below the bolt (LLF). See Figure 2 (D–F) for location of the leafy bracts. All material was flash frozen in liquid nitrogen for storage at −80°C preceding extraction and analysis.

AN and AA Feedback Studies

A. annua was sown from seed in Metromix 360 Soil (Sungro) and grown under continuous light for 14 weeks. Plants of approximately the same height were selected for all treatments. The 10th and 11th leaves from the shoot apical meristem were sprayed with either 100 μg mL^{-1} AN or 100 μg mL^{-1} AA in 70% ethanol; controls were sprayed with 70% ethanol. After 24 h, leaf tissue was harvested for RNA isolation and RT-PCR.

RNA Isolation and Real-Time RT-PCR

Methods briefly described here are detailed by Arsenault et al. (2010). Immediately after harvest, plant samples were flash frozen in liquid nitrogen, ground, and RNA extracted and purified. RNA transcripts were reverse transcribed into cDNA and then analyzed by real-time PCR. Primers were designed for the seven genes using PrimerSelect (Lasergene; DNAStar) based on cDNA sequences specific for *A. annua* available at the National Center for Biotechnology Information (Supplemental Table S1). Primer pairs were designed with similar melting temperatures, to amplify 200- to 300-bp fragments, and checked for amplification and specificity by gel electrophoresis of RT-PCR products. Relative fold changes in gene expression were calculated based on the $2^{-\Delta\Delta CT}$ comparative method (Livak and Schmittgen, 2001; Sehringer et al., 2005; Cikos et al., 2007). Product integrity was checked via melt-curve analysis using the myIQ software package (Bio-Rad).

AN and Artemisinic Precursor Quantification

AN and its metabolites, AA, AB, and DHAA, were extracted from freshly harvested tissues and measured by liquid chromatography-mass spectrometry as described by Mannan et al. (2009). Briefly, tissues were extracted by sonication in toluene, semipurified on a silica gel column, and dried under a stream of nitrogen gas before being resuspended in the liquid chromatography mobile phase (95% acetonitrile + 5 mM ammonium formate). Metabolites

were detected using an atmospheric pressure-electrospray ionization source in single ion monitoring mode for relevant molecular ions, and identity was verified using the spectra and retention times of authentic external standards.

Glandular Trichome and Epidermal Cell Measurements

Glandular trichomes were counted using the method of Lommen et al. (2006). Briefly, terminal leaflets of fully expanded leaves were fixed to glass slides with double-sided adhesive tape. Trichomes were counted using a binocular microscope at 100× magnification within a 10 × 10 grid corresponding to 1 mm^2. Counts were taken twice per leaf at random locations across the surface and averaged for each biological repeat; at least four leaves were measured per condition. Subsequent to trichome counts, epidermal cells were counted using the technique of Capellades et al. (1990). The same leaf sections were then coated with a thin layer of clear nail enamel and allowed to dry completely. The epidermal layer was then peeled off the leaves using clear adhesive tape that was then adhered to a new slide and visualized at 400× magnification with a 10 × 10 grid corresponding to 0.25 mm^2. Epidermal cells within each grid were counted using the same method as trichomes, with the average of two counts per leaf acting as a single replicate using a total of four leaves.

Statistical Analyses

Experiments were independently replicated at least three times, and significant differences in metabolite concentration and trichome density were evaluated using Student's *t* test. The quantitative PCR data were analyzed using the Mann-Whitney *U* test (Yuan et al., 2006).

Supplemental Data

The following materials are available in the online version of this article.

Supplemental Figure S1. Trichome populations on leaves relative to leaf position, surface, and developmental stage.

Supplemental Table S1. Primer sequences.

ACKNOWLEDGMENTS

We greatly appreciate the technical advice and assistance of Prof. Carol Cramer and Dr. Giuliana Medrano of the Arkansas Bioscience Institute. We also appreciate the suggestion of an anonymous reviewer who suggested experiments to test the effects of exogenous AN on transcript levels.

Received July 9, 2010; accepted August 16, 2010; published August 19, 2010.

LITERATURE CITED

Acton N, Klayman DL (1985) Artemisitene, a new sesquiterpene lactone endoperoxide from *Artemisia annua*. Planta Med **51:** 441–442

Arsenault PR, Vail D, Wobbe KK, Weathers PJ (2010) Effect of sugars on artemisinin production in *Artemisia annua* L.: transcription and metabolite measurements. Molecules **15:** 2302–2318

Arsenault PR, Wobbe KK, Weathers PJ (2008) Recent advances in artemisinin production through heterologous expression. Curr Med Chem **15:** 2886–2896

Bhattarai A, Ali AS, Kachur SP, Martensson A, Abbas AK, Khatib R, Al-Mafazy AW, Ramsan M, Rotllant G, Gerstenmaier JF, et al (2007) Impact of artemisinin-based combination therapy and insecticide-treated nets on malaria burden in Zanzibar. PLoS Med **4:** e309

Bouwmeester HJ, Wallaart TE, Janssen MH, van Loo B, Jansen BJ, Posthumus MA, Schmidt CO, De Kraker JW, Konig WA, Franssen MC (1999) Amorpha-4,11-diene synthase catalyses the first probable step in artemisinin biosynthesis. Phytochemistry **52:** 843–854

Brown GD, Sy LK (2007) *In vivo* transformations of artemisinic acid in *Artemisia annua* plants. Tetrahedron **63:** 9548–9566

Capellades M, Fontarnau R, Carulla C, Debergh P (1990) Environment influences anatomy of stomata and epidermal cells in tissue-cultured *Rosa multiflora*. J Am Soc Hortic Sci **115:** 141–145

Chen DH, Ye HC, Li GF (2000) Expression of a chimeric farnesyl diphosphate synthase gene in *Artemisia annua* L. transgenic plants via *Agrobacterium tumefaciens*-mediated transformation. Plant Sci **155:** 179–185

Chien JC, Sussex IM (1996) Differential regulation of trichome formation on the adaxial and abaxial leaf surfaces by gibberellins and photoperiod in *Arabidopsis thaliana* (L.). Plant Physiol **111:** 1321–1328

Cikos S, Bukovska A, Koppel J (2007) Relative quantification of mRNA: comparison of methods currently used for real-time PCR data analysis. BMC Mol Biol **8:** 113

Covello PS, Teoh KH, Polichuk DR, Reed DW (2008) Making artemisinin. Phytochemistry **69:** 2881–2885

Duke SO, Vaughn KC, Croom EM, El Sohly HN (1987) Artemisinin, a constituent of annual wormwood (*Artemisia annua*), is a selective phytotoxin. Weed Sci **35:** 499–505

Efferth T, Marschall M, Wang X, Huong SM, Hauber I, Olbrich A, Kronschnabl M, Stamminger T, Huang ES (2002) Antiviral activity of artesunate toward wild-type, recombinant, and ganciclovir-resistant human cytomegaloviruses. J Mol Med (Berl) **80:** 233–242

Ferreira JFS, Simon JE, Janick J (1995) Developmental studies of *Artemisia annua*: flowering and artemisinin production under greenhouse and field conditions. Planta Med **61:** 167–170

Fung PK, Krushkal J, Weathers PJ (2010) Computational analysis of the evolution of 1-deoxy-D-xylulose-5-phosphate reductoisomerase an important enzyme in plant terpene biosynthesis. Chem Biodivers **7:** 1098–1110

Graham IA, Besser K, Blumer S, Branigan CA, Czechowski T, Elias L, Guterman I, Harvey D, Isaac PG, Khan AM, et al (2010) The genetic map of *Artemisia annua* L. identifies loci affecting yield of the antimalarial drug artemisinin. Science **327:** 328–331

Hsu E (2006) The history of qing hao in the Chinese *materia medica*. Trans R Soc Trop Med Hyg **100:** 505–508

Liu S, Tian N, Li J, Huang J, Liu Z (2009) Isolation and identification of novel genes involved in artemisinin production from flowers of *Artemisia annua* using suppression subtractive hybridization and metabolite analysis. Planta Med **75:** 1542–1547

Livak KJ, Schmittgen TD (2001) Analysis of relative gene expression data using real-time quantitative PCR and the 2 2ΔΔCT method. Methods **25:** 402–408

Lommen WJ, Shenk E, Bouwmeester HJ, Verstappen FW (2006) Trichome dynamics and artemisinin accumulation during development and senescence of *Artemisia annua* leaves. Planta Med **72:** 336–345

Ma C, Wang H, Lu X, Xu G, Liu B (2008) Metabolic fingerprinting investigation of *Artemisia annua* L. in different stages of development by gas chromatography and gas chromatography-mass spectrometry. J Chromatogr A **1186:** 412–419

Mannan A, Liu C, Arsenault P, Towler M, Vail D, Lorence A, Weathers P (2009) DMSO triggers the generation of ROS leading to an increase in artemisinin and dihydroartemisinic acid in *Artemisia annua* shoot cultures. Plant Cell Rep **29:** 143–152

Olsson ME, Olofsson LM, Lindahl AL, Lundgren A, Brodelius M, Brodelius PE (2009) Localization of enzymes of artemisinin biosynthesis to the apical cells of glandular trichomes of *Artemisia annua* L. Phytochemistry **70:** 1123–1128

Picaud S, Olofsson L, Brodelius M, Brodelius PE (2005) Expression, purification, and characterization of recombinant amorpha-4,11-diene synthase from *Artemisia annua* L. Arch Biochem Biophys **436:** 215–226

Ro DK, Paradise EM, Ouellet M, Fisher KJ, Newman KL, Ndungu JM, Ho KA, Eachus RA, Ham TS, Kirby J, et al (2006) Production of the antimalarial drug precursor artemisinic acid in engineered yeast. Nature **440:** 940–943

Romero MR, Efferth T, Serrano MA, Castano B, Macias RI, Briz O, Marin JJ (2005) Effect of artemisinin/artesunate as inhibitors of hepatitis B virus production in an "*in vitro*" replicative system. Antiviral Res **68:** 75–83

Schramek N, Wang H, Römisch-Margl W, Keil B, Radykewicz T, Winzenhörlein B, Beerhues L, Bacher A, Rohdich F, Gershenzon J, et al (2010) Artemisinin biosynthesis in growing plants of Artemisia annua: a $^{13}CO_2$ study. Phytochemistry **71:** 179–187

Sehringer B, Zahradnik HP, Deppert WR, Simon M, Noethling C, Schaefer WR (2005) Evaluation of different strategies for real-time RT-PCR expression analysis of corticotropin-releasing hormone and related proteins in human gestational tissues. Anal Bioanal Chem **383:** 768–775

Singh NP, Lai HC (2004) Artemisinin induces apoptosis in human cancer cells. Anticancer Res **24:** 2277–2280

Sy LK, Brown GD (2002) The mechanism of the spontaneous autoxidation of dihydroartemisinic acid. Tetrahedron **58:** 897–908

Telfer A, Bollman KM, Poethig RS (1997) Phase change and the regulation of trichome distribution in *Arabidopsis thaliana*. Development **124:** 645–654

Tellez MR, Canel C, Rimando AM, Duke SO (1999) Differential accumulation of isoprenoids in glanded and glandless *Artemisia annua*. L. Photochemistry **52:** 1035–1040

Teoh KH, Polichuk DR, Reed DW, Covello PS (2009) Molecular cloning of an aldehyde dehydrogenase implicated in artemisinin biosynthesis in *Artemisia annua*. Botany **87:** 635–642

Teoh KH, Polichuk DR, Reed DW, Nowak G, Covello PS (2006) *Artemisia annua* L. (Asteraceae) trichome-specific cDNAs reveal CYP71AV1, a cytochrome P450 with a key role in the biosynthesis of the antimalarial sesquiterpene lactone artemisinin. FEBS Lett **580:** 1411–1416

Towler MJ, Weathers PJ (2007) Evidence of artemisinin production from IPP stemming from both the mevalonate and the nonmevalonate pathways. Plant Cell Rep **26:** 2129–2136

Utzinger J, Keiser J (2004) Schistosomiasis and soil-transmitted helminthiasis: common drugs for treatment and control. Expert Opin Pharmacother **5:** 263–285

Wallaart TE, Bouwmeester HJ, Hille J, Poppinga L, Maijers NC (2001) Amorpha-4,11-diene synthase: cloning and functional expression of a key enzyme in the biosynthetic pathway of the novel antimalarial drug artemisinin. Planta **212:** 460–465

Wang H, Ge L, Ye HC, Chong K, Liu BY, Li GF (2004) Studies of the effects of fpf1 gene on *Artemisia annua* flowering time and on the linkage between flowering and artemisinin biosynthesis. Planta Med **70:** 347–352

Woerdenbag HJ, Luers J, van Uden W, Pras N, Malingre T, Alfermann A (1993) Production of the new antimalarial drug artemisinin in shoot cultures of *Artemisia annua* L. Plant Cell Tissue Organ Cult **32:** 247–257

Yuan JS, Reed A, Chen F, Stewart CNJ (2006) Statistical analysis of real-time PCR data. Bioinformatics **7:** 85–90

Zhang L, Ye HC, Li GF (2006) Effect of development state on the artemisinin content and the sequence characterized amplified region (SCAR) marker of high-artemisinin yielding strains of *Artemisia annua* L. J Integr Plant Biol **48:** 1054–1062

Zhang Y, Teoh KH, Reed DW, Covello PS (2009) Molecular cloning and characterization of Dbr1, a 2-alkenal reductase from *Artemisia annua*. Botany **87:** 643–649

Zhang Y, Teoh KH, Reed DW, Maes L, Goossens A, Olson DJ, Ross AR, Covello PS (2008) The molecular cloning of artemisinic aldehyde Δ11(13) reductase and its role in glandular trichome-dependent biosynthesis of artemisinin in *Artemisia annua*. J Biol Chem **283:** 21501–21508

Zhang YS, Ye HC, Liu BY, Wang H, Li GF (2005) Exogenous GA3 and flowering induce the conversion of artemisinic acid to artemisinin in *Artemisia annua* plants. Russ J Plant Physiol **52:** 58–62